4 Biaxial Stretching of a Rubber Membrane – A Paradigm of Stability, Symmetry-Breaking, and Hysteresis

4.1 Load-Deformation Relations of a Biaxially Loaded Mooney-Rivlin Membrane

An elastic bar shortens under compression. But, if the compressive force surpasses a critical value, the bar buckles and so does an elastic sheet. This happens for all elastic materials, also for rubber. We learn about this phenomenon as students in a course usually called Strength of Materials, and we have thus come to associate buckling with compression. In rubber, however, *buckling can occur in tension*, and that is what we shall investigate in this chapter. The instability of an elastic rubber sheet under tension was first discovered by Kearsley.

Maybe we should not call the phenomenon "buckling" when it occurs in tension – and we will not do so in the sequel – but the fact remains that for a rubber membrane under tension there is a critical load where two competing solutions exchange stability, just like in buckling. Let us consider the following:

As in Fig. 2.5 we apply loads $\bar{P}_\lambda$ and $\bar{P}_\mu$ quasistatically to the edges of a rubber membrane, whose stress-stretch relation is given by (3.19). We introduce the constant $K = \frac{s_+}{|s_-|}$, which – according to (3.16) – we take to have the value 10. Also we use $|s_-|$ to introduce the dimensionless elastic forces

$$\begin{aligned} \bar{F}_\lambda &= \tfrac{1}{|s_-|}\tfrac{t_{\lambda\lambda}}{\lambda} = \left(\lambda - \tfrac{1}{\lambda^3\mu^2}\right)\left(K + \mu^2\right) \quad \text{and} \\ \bar{F}_\mu &= \tfrac{1}{|s_-|}\tfrac{t_{\mu\mu}}{\mu} = \left(\mu - \tfrac{1}{\mu^3\lambda^2}\right)\left(K + \lambda^2\right). \end{aligned} \tag{4.1}$$

These two equations represent the force-stretch relations of a biaxially loaded Mooney-Rivlin membrane.

4.2 Deformation of a Square Membrane Under Symmetric Loading

We imagine a *square* membrane whose undistorted lengths L^0_λ and L^0_μ are equal and we ask how it deforms under equal loads $\bar{F}_\lambda = \bar{F}_\mu$. By (4.1) the deformations λ and μ must then satisfy the condition

I. Müller and P. Strehlow: *Rubber and Rubber Balloons, Paradigms of Thermodynamics*, Lect. Notes Phys. **637**, (2004), pp. 35–50
http://www.springerlink.com/

$$\left(\lambda - \frac{1}{\lambda^3\mu^2}\right)\left(K + \mu^2\right) = \left(\mu - \frac{1}{\mu^3\lambda^2}\right)\left(K + \lambda^2\right) \tag{4.2}$$

which may be written in the form

$$(\lambda - \mu)\left\{\left(\lambda^3\mu^3 + 1\right)K + \left(\lambda^2 + \lambda\mu + \mu^2 - \lambda^4\mu^4\right)\right\} = 0. \tag{4.3}$$

Obviously this condition permits equal deformations $\lambda = \mu$ in both directions, so that the square membrane remains square irrespective of the size of the deformation. This is, in fact, the solution which we expect to see on intuitive grounds for equal loading. It is a universal solution, since it does not depend on a material parameter.

However, there is a second solution of (4.3), for which the curly bracket vanishes. This condition determines λ in terms of μ as the solution of an algebraic equation of fourth order. The only real root $\lambda(\mu)$ with λ and μ both positive is represented by the hyperbola-shaped graph in Fig. 4.1. The figure also shows the symmetric solution $\lambda = \mu$.

Inspection shows that for each μ there are two possible values of λ , and *vice versa*. One of those is equal to μ while the other one is not. The two graphs intersect at $\lambda = \mu \approx 3.17$ and, by (4.1), the corresponding (non-dimensional) forces are $\bar{F}_\lambda = \bar{F}_\mu = 63.43$.

Only the symmetric solution passes through the undistorted state $\lambda = \mu = 1$ with $\bar{F}_\lambda = \bar{F}_\mu = 0$. It follows that upon gradual biaxial loading with $\bar{F}_\lambda = \bar{F}_\mu$ – starting in the undistorted state – the membrane has no choice but to follow the symmetric solution until the equal loads reach $\bar{F}_\lambda = \bar{F}_\mu = 63.43$. Here we meet a bifurcation of the solution curve and

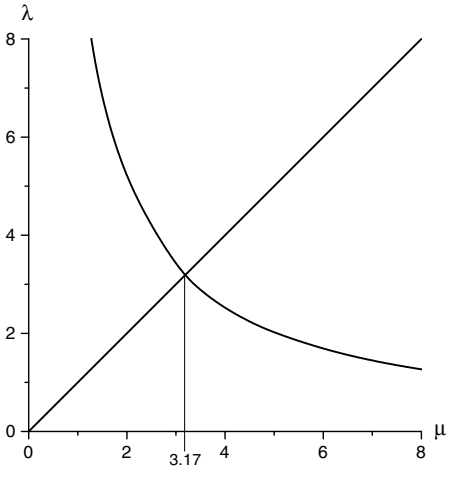

Fig. 4.1. Deformations λ and μ for a symmetrically loaded square membrane. The graphs represent the solutions of (4.3) for K =10. The point of intersection is $\lambda = \mu \approx 3.17$

the membrane will subsequently – upon further loading – follow the *stable* curve. We have yet to determine which curve that is, see Sect. 4.4 below.

Note that the non-symmetric solution $\lambda(\mu)$ defined by the vanishing of the curly bracket in (4.3) is obviously not universal, since it contains the material coefficient K. Indeed, the equation for $\lambda(\mu)$ may be written in the form

$$K=\frac{\lambda^4\mu^4-\left(\lambda^2+\lambda\mu+\mu^2\right)}{\lambda^3\mu^3+1}. \tag{4.4}$$

The right-hand-side of this equation is clearly smaller than $\lambda\mu$. It follows that this non-symmetric solution cannot exist for pairs λ, μ for which $\lambda\mu$ is smaller or equal to K. In particular, therefore, for a neo-Hookean material, where K is infinity, we expect to see only the symmetric solution.

4.3 Stability Criteria

Mechanics proper has no stability criterion. Indeed, when mechanicians speak about stability, they borrow their criterion from thermodynamics, which is the only branch of science with a natural inequality. We proceed to derive the stability condition for the square membrane, limiting the attention to the case of uniform and constant temperature T.

Starting points are the first and second laws of thermodynamics applied to the membrane, viz.

$$\frac{\mathrm{d}(U+K)}{\mathrm{d}t}=\dot{Q}+\dot{W} \quad \text{and} \quad \frac{\mathrm{d}S}{\mathrm{d}t}\geq\frac{\dot{Q}}{T}. \tag{4.5}$$

$\dot{W}$ is the working of the applied loads, namely

$$\dot{W}=P_\lambda\frac{\mathrm{d}L_\lambda}{\mathrm{d}t}+P_\mu\frac{\mathrm{d}L_\mu}{\mathrm{d}t}. \tag{4.6}$$

Although these equations are superficially similar to those utilized before, e.g. in Sects. 2.1 and 2.7, they are in fact quite different. First of all, the second law is now given by an *inequality* indicating that we expect a non-zero entropy production or dissipation. The idea is that the loads may be applied suddenly, rather than quasistatically. Therefore the loads P_λ and P_μ are not equilibrated by the elastic forces $\bar{P}_\lambda=\frac{\partial F}{\partial L_\lambda}$ and $\bar{P}_\mu=\frac{\partial F}{\partial L_\mu}$. The initial stretches inside the membrane may be strongly inhomogeneous; accelerations occur everywhere and the kinetic energy K of the membrane is not negligible.

Yet we may still eliminate $\dot{Q}$ and $\dot{W}$ between (4.5) and (4.6) and obtain

$$\frac{\mathrm{d}(U-TS+K)}{\mathrm{d}t}\leq P_\lambda\frac{\mathrm{d}L_\lambda}{\mathrm{d}t}+P_\mu\frac{\mathrm{d}L_\mu}{\mathrm{d}t}. \tag{4.7}$$

Thus, whatever the initial state of the membrane was, and however we change its lengths L_λ, L_μ as functions of time, or whichever loads P_λ, P_μ we bring to bear, the inequality (4.7) must be satisfied.

There are two instructive special cases in which we expect that eventually an equilibrium will be reached. Those are the cases of *clamping* and of *dead-loading*.

Clamping of the membrane means that L_λ and L_μ are fixed, i.e. constant in time. Under these circumstances we have

$$\frac{\mathrm{d}(U - TS + K)}{\mathrm{d}t} \leq 0 \tag{4.8}$$

and experience tells us that the initially arbitrarily moving and deforming membrane will come to rest in a homogeneous state of equilibrium. According to (4.8) this homogeneous state is characterized by a minimal free energy F. Thus

$$F = U - TS \sim \text{ minimal} \tag{4.9}$$

is the stability criterion for a clamped body.

Dead-loading means that the loads P_λ, P_μ are fixed. In that case (4.7) implies

$$\frac{\mathrm{d}(U - TS + K - P_\lambda L_\lambda - P_\mu L_\mu)}{\mathrm{d}t} \leq 0. \tag{4.10}$$

We expect that the membrane will approach a homogeneous state of rest as equilibrium is approached and that state, by (4.10), is characterized by a minimal free enthalpy − or Gibbs free energy G. We thus have

$$G = U - TS - P_\lambda L_\mu - P_\mu L_\mu \sim \text{ minimal} \tag{4.11}$$

as the stability criterion for a dead-loaded body.

Note that since P_λ and P_μ are constant, G is a function of L_λ and L_μ. A necessary condition for G to be minimal in equilibrium – index E – is therefore

$$P_\lambda^{\mathrm{E}} = \tfrac{\partial F}{\partial L_\lambda} = \bar{P}_\lambda \quad \text{and} \quad P_\mu^{\mathrm{E}} = \tfrac{\partial F}{\partial L_\mu} = \bar{P}_\mu.$$

Thus in equilibrium the applied loads are equilibrated by the elastic forces $\bar{P}_\lambda$ and $\bar{P}_\mu$ which are derivatives of the free energy F. We have anticipated this relation in previous chapters and sections when dealing with quasistatic processes.

4.4 Minimal Free Energy

We proceed to use the clamping criterion of free energy to determine the stability of the square membrane under symmetric loading for which we have

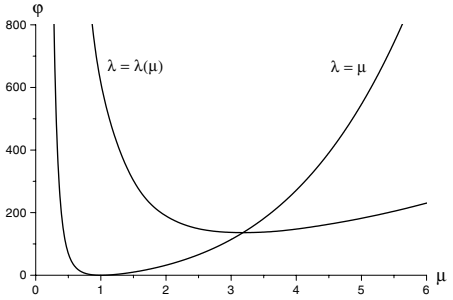

Fig. 4.2. Free energy densities φ for the symmetric and asymmetric solutions

found two solutions, cf. Fig. 4.1. The free energy of a membrane with stretches λ and μ is given in (3.22) which we rewrite here in a dimensionless form

$$\varphi = \frac{U-TS}{|s_-|V} = \frac{1}{2}K\left(\lambda^2+\mu^2+\frac{1}{\lambda^2\mu^2}-3\right)+\frac{1}{2}\left(\frac{1}{\lambda^2}+\frac{1}{\mu^2}+\lambda^2\mu^2-3\right). \quad (4.12)$$

Since we consider clamping the membrane, we expect an equilibrium for any arbitrary pair (λ, μ). But we are interested in the relative stability of the symmetric and non-symmetric deformations of Fig. 4.1, $\lambda = \mu$ and $\lambda = \lambda(\mu)$ respectively. In other words we are interested in clamps for pairs (λ, μ) which can be maintained by equal loads $F_\lambda = F_\mu$.

Therefore we plot the function $\varphi(\lambda, \mu)$ as a function of μ along the two curves $\lambda = \mu$ and $\lambda(\mu)$ which represent possible deformations for the symmetrically loaded membrane. The result is shown in Fig. 4.2. Inspection shows that for $\mu < 3.17$ the symmetric solution has a smaller energy, while for $\mu > 3.17$ this is true for the asymmetric solution. We conclude that the symmetric solution loses stability at the bifurcation point. We recall that this point corresponds to the *critical* (non-dimensional) loads $F_\lambda = F_\mu = 63.43$. When those loads are surpassed the hitherto square membrane becomes rectangular. At the bifurcation point a random fluctuation will decide whether the long side of the rectangle is in the λ- or μ-direction.

4.5 Free Enthalpy, Gibbs Free Energy

The competition between the two deformations of the square membrane, − the symmetric one and the unsymmetric one − may also be read off from the free enthalpies. In order to see this we plot the free enthalpy (4.11), or its dimensionless density

$$\gamma = \varphi - F_\lambda\lambda - F_\mu\mu$$

$$\gamma = \frac{1}{2}K\left(\lambda^2+\mu^2+\frac{1}{\lambda^2\mu^2}-3\right)+\frac{1}{2}\left(\frac{1}{\lambda^2}+\frac{1}{\mu^2}+\lambda^2\mu^2-3\right)-F_\lambda\lambda-F_\mu\mu, \quad (4.13)$$

for equal (non-dimensional) loads $F_\lambda = F_\mu = F$ and for the two solutions $\lambda = \mu$ and $\lambda = \lambda(\mu)$, cf. Fig. 4.1. For four values of F we obtain the graphs of Fig. 4.3.

Inspection of Fig. 4.3 shows that for small loads F the symmetric solution has a lower minimum of the free enthalpy γ than the asymmetric one. In particular this is true for $F = 0$, where the low minimum lies in the undistorted state $\mu = \lambda = 1$. As F grows this situation remains unchanged except that the equilibrium stretches $\mu = \lambda$ grow to assume values larger than one. For $F = 63.43$ the equilibrium value lies at $\mu = \lambda = 3.17$ and in that critical case both curves − the free enthalpies for the symmetric and for the asymmetric solution − have a minimum at the same point. For still larger values of F the "asymmetric curve" develops two minima and both have a smaller value than the minimum of the "symmetric curve". For $F = 90$ the two minima occur at $\mu = 1.31$ and $\mu = 7.68$ and they correspond to λ-values $\lambda = 7.68$ and $\lambda = 1.31$ respectively. Thus we confirm that at the critical load $F = 63.43$ there is an exchange of stability from the symmetric solution to the asymmetric one. In the present case, where the loads are fixed, the stable situations are characterized by exhibiting minima of the free enthalpy γ.

Another aspect of this situation − maybe a more suggestive one − reveals itself when we plot the free enthalpy (4.13) for $F_\lambda = F_\mu = F$ as a function of λ and μ. The easiest way to represent that function is by drawing contour lines and they are shown in the two graphs of Fig. 4.4. The left hand side refers to the subcritical load $F = 20$ and, as expected, we see that the minimum lies on the bisector, namely at a point $\lambda = \mu = 1.65 < 3.17$. But the right hand side of Fig. 4.4, for the supercritical load $F = 70$, shows a saddle on the bisector and two minima situated symmetrically on either side at $(\lambda, \mu) = (2.02, 4.97)$ and $(4.97, 2.02)$.

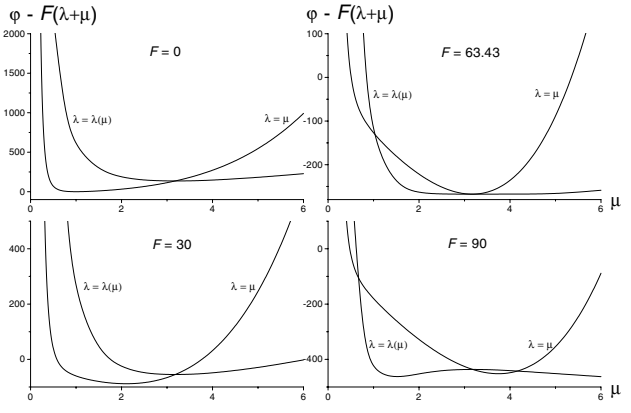

Fig. 4.3. Free enthalpy densities γ for symmetric loading with forces $F_\lambda = F_\mu = F$. $\lambda = \mu$: symmetric solution, $\lambda = \lambda(\mu)$: asymmetric

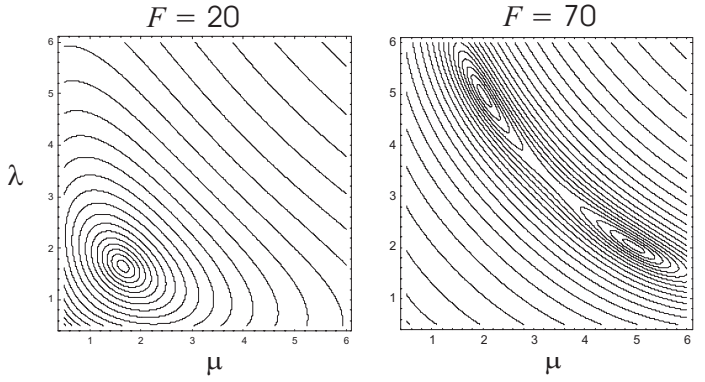

Fig. 4.4. Contour lines of free enthalpy density $\gamma = \varphi - F(\lambda + \mu)$ for a subcritical load $F = 20$ (left) and for a supercritical one $F = 70$ (right)

4.6 Symmetry Breaking

It is instructive to investigate the case when the forces F_λ and F_μ are unequal, albeit by a small amount only. We set $F_\lambda = \zeta F_\mu$ and choose $\zeta < 1$ so that the load in the μ-direction is now bigger than in the λ-direction. The equations (4.1) are still valid, but instead of (4.2) we now obtain

$$\left(\lambda - \frac{1}{\lambda^3 \mu}\right)\left(K + \mu^2\right) = \zeta \left(\mu - \frac{1}{\mu^3 \lambda^2}\right)\left(K + \lambda^2\right). \tag{4.14}$$

In this case − unlike before − it is impossible to factorize the expression and thus obtain one easy universal solution. We have to solve the full algebraic equation of fifth order for λ, viz.

$$\lambda^5 - \frac{1}{\zeta}\left(\mu + \frac{K}{\mu}\right)\lambda^4 - \left(\frac{1}{\mu^4} - K\right)\lambda^3 - \frac{K}{\mu^4}\lambda + \frac{1}{\zeta}\left(\frac{1}{\mu} + \frac{K}{\mu^3}\right) = 0. \tag{4.15}$$

It is still true that there are only two real solutions with λ and μ positive and Fig. 4.5 shows us their numerically calculated graphs, always for $K = 10$ and for three different values of ζ smaller than 1 as indicated.

Inspection shows that the bifurcation which occurs in the symmetric case $\zeta = 1$ vanishes for asymmetric loads. The two intersecting graphs for $\zeta = 1$ are now separated and recombined so that their upper and lower parts form two smooth curves with a gap in-between, where the bifurcation point used to be. The gap becomes more pronounced when the loading becomes more and more asymmetric. It is still true that λ and μ jointly grow away from 1 as the loads are increased, but then a maximum is reached and λ actually decreases while μ increases strongly. The bias toward μ results, of course, from the fact that $F_\mu > F_\lambda$ holds.

This is an instructive example of the phenomenon of symmetry breaking: As long as the loads are applied symmetrically there is a non-uniqueness in

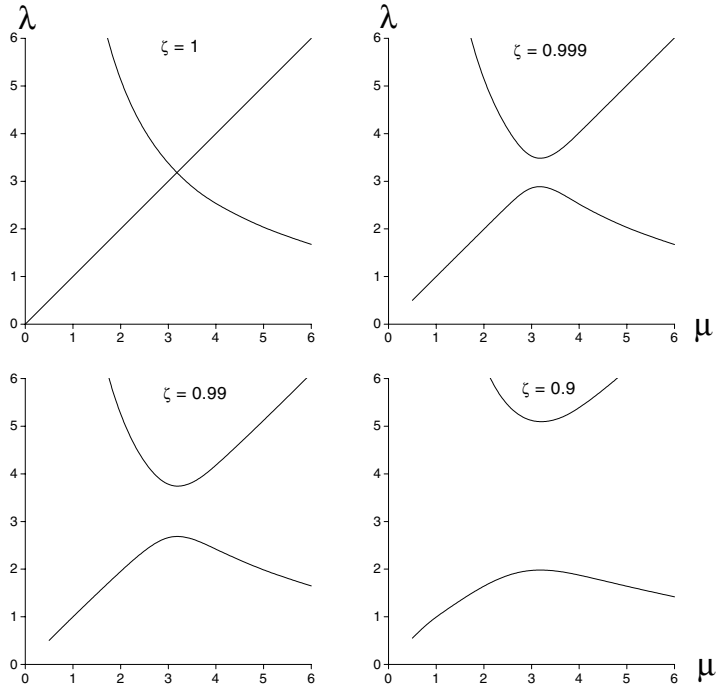

Fig. 4.5. λ as a function of μ for symmetric and asymmetric loads

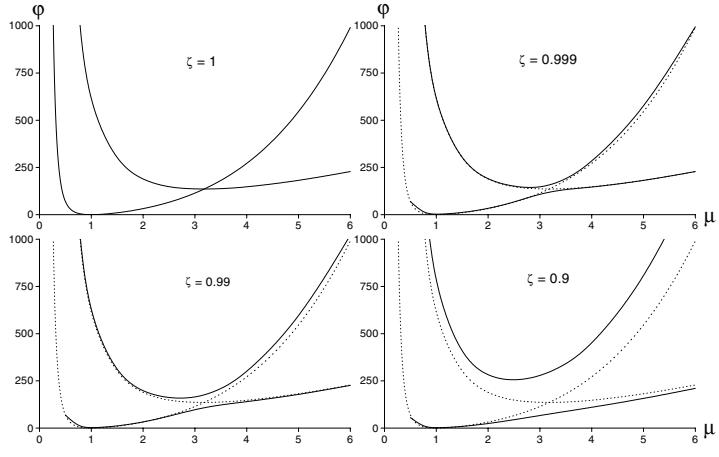

Fig. 4.6. Free energy φ as function of μ for symmetric and asymmetric loads

the solution, i.e. a bifurcation occurs and the choice of deformation is left to random fluctuations. But once the symmetry is "broken", i.e. unequal loads are applied − however close in value − the bifurcation vanishes and the subsequent deformations are uniquely determined.

The separation and recombination of the graphs $\lambda(\mu)$ which is associated with the symmetry-breaking has its counterpart in the free energy curves. This fact is demonstrated in Fig. 4.6. In each graph of that figure we have indicated by dotted lines the original curves for the case of symmetric loading. This helps us to understand to what extent the symmetry breaking has altered the situation.

4.7 Hysteresis

We continue to consider asymmetric loads and plot the free enthalpy $\gamma = \varphi - F_\lambda\lambda - F_\mu\mu$, cf. (4.13) for $F_\lambda = 10$ and $F_\mu = 20$. Figure 4.7 shows the contour lines and we recognize a minimum slightly off the bisector in the μ-direction, because $F_\mu > F_\lambda$ holds; both loads are far below the critical value.

The picture changes drastically when we proceed to higher loads, where we expect the possibility of two minima. Figure 4.8 represents an instructive visualization of the free enthalpy in that case. All six diagrams of the figure refer to $F_\mu = 70$, but F_λ changes from the value 75 down to 65.

$F_\lambda = 75$ is sufficiently larger than F_μ that there is only one minimum for large λ and small μ. For $F_\lambda = 70.7$ a second minimum has appeared which would favour μ over λ, but this new minimum lies higher than the first one and − more importantly − it is cut off from it by a barrier. The rectangular membrane will thus remain with the long side in the λ-direction. The same is true for $F_\lambda = 70.3$ and even for $F_\lambda = 69.7$ and $F_\lambda = 69.3$ although for the latter two values the second minimum is deeper than the first one, but still the barrier prevents the transition. In fact, the transition to the right

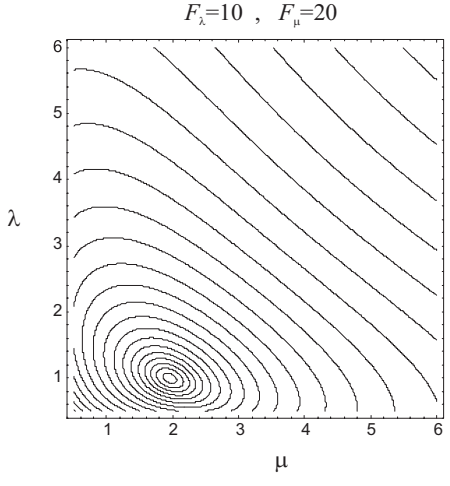

Fig. 4.7. Contour lines of free enthalpy density $\gamma = \varphi - F_\lambda\lambda - F_\mu\mu$ for $F_\lambda = 10$, $F_\mu = 20$, both subcritical

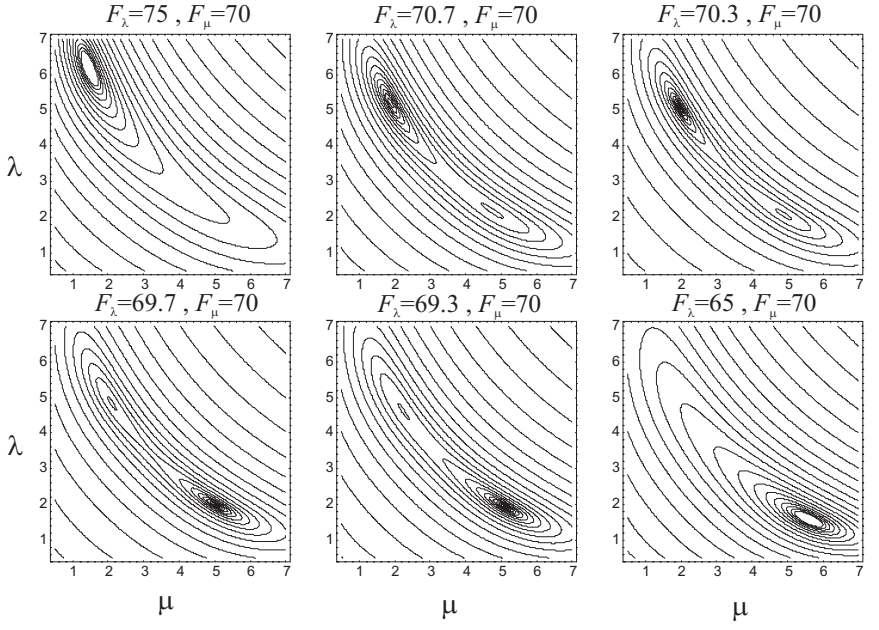

Fig. 4.8. Possibility of hysteretic behaviour of the membrane in a loading-unloading cycle of F_λ for fixed F_μ

minimum with the longer edge in the μ-direction will only occur somewhere between $F_\lambda = 69.3$ and $F_\lambda = 65$, namely when the left minimum disappears and the barrier is eliminated.

Upon increasing F_λ again that newly created state will persist until the right minimum is eliminated somewhere between $F_\lambda = 70.7$ and $F_\lambda = 75$. Thus we conclude that a loading-unloading cycle of F_λ will be hysteretic and we proceed to describe that hysteretic behaviour of the membrane more directly.

4.8 Non-monotone Force-Stretch Relation

If we apply a dead load F_λ^0 in the λ-direction which we fix once and for all, we can come close to a uniaxial force-stretch characteristic of a tensile specimen by gradually increasing $\bar{F}_\mu$ and plotting it against the deformation μ. Fixing F_λ to the value F_λ^0 provides us with a biquadratic equation for μ in terms of λ by rewriting $(4.1)_1$. We thus obtain

$$\mu^2 = \frac{1}{2}\left(\frac{F_\lambda^0}{\lambda} + \frac{1}{\lambda^4} - K\right) + \sqrt{\frac{1}{4}\left(\frac{F_\lambda^0}{\lambda} + \frac{1}{\lambda^4} - K\right)^2 + \frac{K}{\lambda^4}}. \tag{4.16}$$

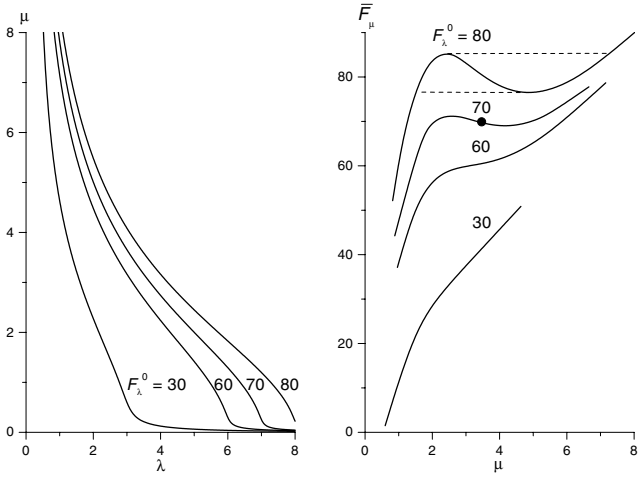

Fig. 4.9. Non-monotonicity and hysteresis. Left: μ as a function of λ for different values of F_λ^0. Right: $\bar{F}_\mu$ as function of μ for different dead loads F_λ^0

For every given F_λ^0 this equation represents a one-to-one relation $\mu = \mu\left(\lambda; F_\lambda^0\right)$, and hence follows by inversion $\lambda = \lambda\left(\mu; F_\lambda^0\right)$. Figure 4.9_{left} shows the (μ, λ)-plot for several values of F_λ^0. The functions $\lambda = \lambda\left(\mu; F_\lambda^0\right)$ are inserted into $(4.1)_2$ and thus we obtain

$$\bar{F}_\mu = \bar{F}_\mu\left(\mu; F_\lambda^0\right). \tag{4.17}$$

It is true that we cannot determine these functions analytically but they are easily found numerically − even with a pocket calculator. Figure 4.9_{right} shows the results for several values of the tensile preload F_λ^0.

All graphs in Fig. 4.9_{right} start with a value $\mu < 1$ for $\bar{F}_\mu = 0$, since the dead load F_λ^0 in the λ-direction causes a lateral contraction in the μ-direction. An increase of $\bar{F}_\mu$ will make μ increase monotonically for the subcritical dead loads $F_\lambda^0 = 30$ and $F_\lambda^0 = 60$. However, for values of F_λ^0 larger than the critical load we observe non-monotonic $\bar{F}_\mu\left(\mu; F_\lambda^0\right)$-curves, which implies that − in a certain range of stretches μ − the force decreases with increasing stretch.

There is a subtle point to be made concerning stability in connection with non-monotonic force-stretch curves of the type shown in Fig. 4.9_{right}. All points on those non-monotonic curves are perfectly stable, if we prescribe and control the stretch μ. The corresponding value $\bar{F}_\mu$ merely provides the value of the force needed to maintain the prescribed stretch.

It is true that the point $\left(F_\lambda^0, \bar{F}_\mu\right) = (70, 70)$, marked by a dot at $\lambda = \mu = 3.326$ in Fig. 4.9_{right}, corresponds to equal stretches λ and μ and therefore it represents a saddle point in the energy plot of Fig. 4.4_{right}. However, since we control μ, there is no way for the membrane to leave this saddle. Much the same holds for the other points on the descending branch of the $\bar{F}_\mu\left(\mu; F_\lambda^0\right)$-

graph in Fig. 4.9. We remind the reader of Buridan's ass who in fact may well be stably shackled to any point between his bales of hay and, in particular, to the mid point. In other words, the "unstable" position in the middle can easily be *stabilized* by the shackles. We thus learn that there is no such thing as an unstable position *per se*. Rather stability of a body or the lack of it must be viewed in terms of the constraints that we can bring to bear on it.

4.9 Hysteresis and Breakthrough. Dissipation

We proceed to emphasize the point just made by looking at the case where Buridan's ass is left unshackled. We do not control the stretch μ any longer, rather we prescribe and control the load F_μ.

We start with $F_\mu = 0$ and slowly increase that force, thereby increasing μ monotonically and quasistatically as long as F_λ^0 is subcritical, i.e. its value is below 63.43, so that the curve $\bar{F}_\mu\left(\mu; F_\lambda^0\right)$ is monotonic. Now, however, let us make F_λ^0 equal to 80 so that the uppermost − non-monotonic − curve of Fig. 4.9 represents the relevant force-stretch graph $\bar{F}_\mu\left(\mu; F_\lambda^0\right)$. As soon as the applied load F_μ exceeds the maximum of that curve there will be a horizontal breakthrough until the second ascending branch is reached with a much increased value of μ.

The reverse happens upon unloading: in reverse as soon as the force F_μ falls below the minimum, a horizontal breakthrough occurs which leads us back to the initial ascending branch. The two horizontal breakthrough lines − dashed in Fig. 4.9 − define the upper and lower branches of a hysteresis loop. We call them the yield line and the recovery line, respectively.

It follows that there is no way to enter into the hysteresis loop when we prescribe and control the force F_μ. In particular, we can never reach a point on the descending branch of the $\bar{F}_\mu\left(\mu; F_\lambda^0\right)$ graph.

The breakthrough is interesting from a thermodynamic point of view because it is not a quasistatic process. Rather it is sudden or dissipative or both, meaning that the kinetic energy K, or the non-negative entropy production Σ, or both are not negligible along the breakthrough line. In order to investigate this irreversible process we write the first and second laws in the form, cf. (4.5), (4.6)

$$\frac{\mathrm{d}(U+K)}{\mathrm{d}t} = \dot{Q} + P_\lambda^0 \frac{\mathrm{d}L_\lambda(L_\mu)}{\mathrm{d}t} + P_\mu \frac{\mathrm{d}L_\mu}{\mathrm{d}t} \quad \text{and} \quad \frac{\mathrm{d}S}{\mathrm{d}t} = \frac{\dot{Q}}{T} + \Sigma, \tag{4.19}$$

which is appropriate for a dissipative process with a dead load P_λ^0 in the λ-direction and also loading in the μ-direction so that L_λ becomes a function of L_μ, cf. Fig. 4.9_{left}. As usual we eliminate $\dot{Q}$ and we introduce non-dimensional quantities. Thus for the case under consideration we obtain

$$\frac{\mathrm{d}\left(\varphi\left(\mu, \lambda\left(\mu\right)\right) - F_\lambda^0 \lambda\left(\mu\right)\right)}{\mathrm{d}t} = F_\mu \frac{\mathrm{d}\mu}{\mathrm{d}t} - \frac{\mathrm{d}k}{\mathrm{d}t} - T\sigma. \tag{4.20}$$

k and σ are non-dimensional quantities for kinetic energy and entropy production.

As long as the loading in the μ-direction can proceed quasistatically – i.e. along the ascending branches of the curves $\bar{F}_\mu\left(\mu; F_\lambda^0\right)$ – we may neglect k and σ in (4.20) and obtain

$$\bar{F}_\mu = \frac{\partial\left(\varphi\left(\mu, \lambda\left(\mu\right)\right) - F_\lambda^0 \lambda\left(\mu\right)\right)}{\partial \mu}. \tag{4.21}$$

Thus in this case with a dead load F_λ^0 the quasistatic load $\bar{F}_\mu$ is not only equilibrated by the elastic forces but also by the dead load. The second term in (4.21), the one with F_λ^0, represents the potential energy of that dead load.

But now, what about the breakthrough, where we cannot maintain quasistaticity? We recall (4.21) and write (4.20) in the form

$$\left(F_\mu - \bar{F}_\mu\right)\frac{\mathrm{d}\mu}{\mathrm{d}t} = \frac{\mathrm{d}k}{\mathrm{d}t} + T\sigma, \tag{4.22}$$

whence we conclude that the power of the load F_μ in excess over the quasistatic load $\bar{F}_\mu$ is converted into kinetic energy and/or entropy production.

We may integrate (4.22) along the breakthrough line between times t_0 and t where $\mu(t_0)$ is the abcissa of the maximum, i.e. the initial stretch of the breakthrough. Taking for granted that $k(t_0)$ is zero we get

$$\int_{\mu(t_0)}^{\mu(t)} \left(F_\mu - \bar{F}_\mu\right)\mathrm{d}\mu = k(t) + \int_{t_0}^{t} T\sigma \ \mathrm{d}t. \tag{4.23}$$

Therefore we conclude that the area enclosed between the breakthrough line $F_\mu = const$ and the quasistatic curve $\bar{F}_\mu\left(\mu; F_\lambda^0\right)$ represents the sum of kinetic energy and dissipation created by the irreversible breakthrough. Figure 4.10 illustrates this. The kinetic energy will be found in the form of vibration of the system and the dissipation will usually be felt as heat.

Of course, once the breakthrough line arrives at the stretch μ_E cf. Fig. 4.10, the vibration will gradually die out so that the kinetic energy will again be zero. Thus when the breakthrough is complete, and stationary conditions have returned, the energy

$$\int_{\mu(t_0)}^{\mu_\mathrm{E}} \left(F_\mu - \bar{F}_\mu\right)\mathrm{d}\mu$$

has been dissipated entirely.

4.10 A Three-Dimensional View

An instructive three-dimensional view of the ensemble of curves $\mu\left(\bar{F}_\mu; F_\lambda^0\right)$ in Fig. 4.9_{right} is gained when the graphs are plotted three-dimensionally in a

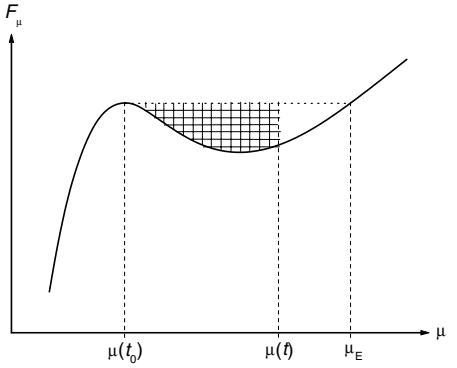

Fig. 4.10. Shaded area equals kinetic energy plus dissipation during breakthrough

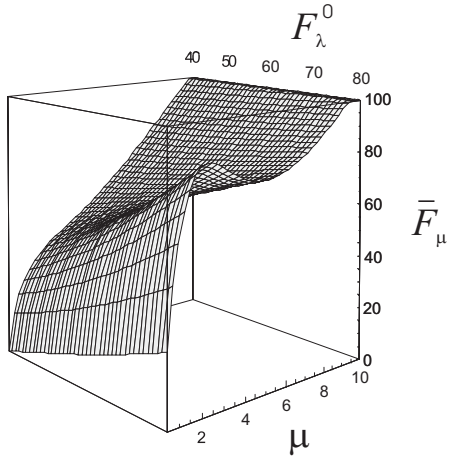

Fig. 4.11. Three-dimensional view of the graphs $\mu = \mu\left(\bar{F}_\mu, F_\lambda^0\right)$ from Fig. 4.9_{right}.

$\left(\mu, \bar{F}_\mu; F_\lambda^0\right)$-diagram, cf. Fig. 4.11. The function $\mu\left(\bar{F}_\mu; F_\lambda^0\right)$ begins to develop a fold at the critical value $F_\lambda^0 = 63.43$ and that fold becomes more pronounced for larger values of F_λ^0.

4.11 Comparison with Treloar's Dead Loading Experiment

According to Fig. 4.9 there are two stable stretches λ and μ for one load $F_\mu = F_\lambda^0$ provided that this load exceeds the critical one, which is equal to 63.43 for $K = 10$. After this non-uniqueness of stretches was discovered by Kearsley he was quick to link it to the different values of λ_1 and λ_2 which Treloar had observed in his biaxial tests, see the table in Fig. 3.8 and the

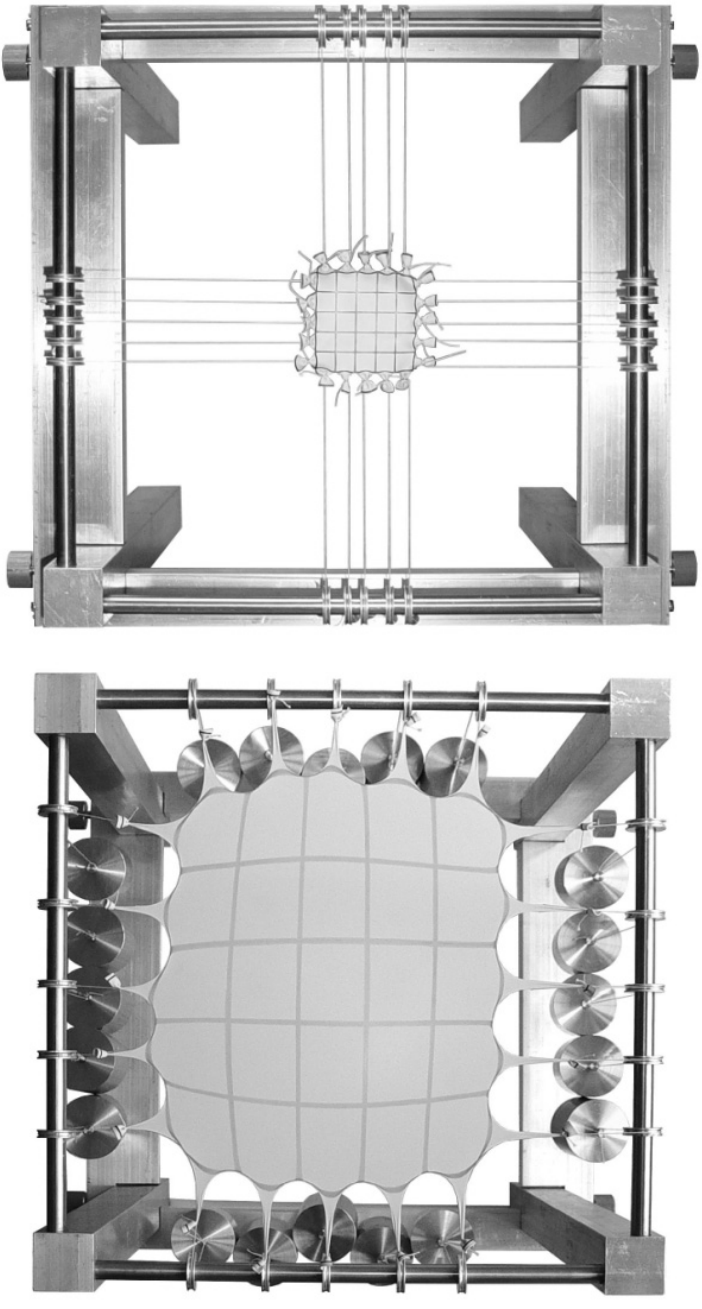

Fig. 4.12. Symmetrically loaded membrane. An experiment

chevrons in Fig. 3.10_{left}. In fact Kearsley considers Treloar's experiments as proof that the "buckling under tension" really does occur and Ericksen calls the phenomenon the "Treloar effect".

Unfortunately, however, this is a misinterpretation of Treloar's results, or an over-interpretation. Indeed, a careful study of Treloar's data shows that his largest load − namely 500 gr − does not even come close to the critical load, where the bifurcation occurs. If we redo the calculation of the present chapter with Treloar's data − and properly convert our units into Treloar's archaic ones − we obtain a critical load of 1125 gr, more than twice as big as Treloar's highest load!

Therefore the "Treloar effect" turns out to be nothing other than one more manifestation of the notorious lack of rubber to provide reproducible and reliable data in a single experiment of large stretch. Reproducible data for strongly stretched rubber usually emerge after "training", i.e. after a specimen has undergone a loading process several times.[1]

4.12 Experimental Evidence for Bifurcation

After Treloar's experiments were recognized as *not* giving evidence for bifurcation of a square membrane, we realized that we would have to do the experiment ourselves if we wanted evidence. This we did and the results of our experiment have confirmed Kearsley's analysis in a satisfactory manner.

Figure 4.12 shows the membrane in the undistorted state (top) and with loads $P_\lambda = P_\mu = 23.3\,\mathrm{N}$ (bottom). We recognize that the initially small central square of dimension $1\,\mathrm{cm} \times 1\,\mathrm{cm}$ has become a large rectangle of dimensions $3.05\,\mathrm{cm} \times 4.06\,\mathrm{cm}$. This is clear evidence that the square shape has lost stability.

Our membrane was characterized by the value $K = 9.60$, so that the critical loads and stretches have the values 23.12 N and 3.106 respectively. Thus the observed post-bifurcation stretches $\lambda = 3.05$ and $\mu = 4.06$, cf. Fig. 4.12, are clearly supercritical.

As an incidental observation we note that at and around the critical load $P_\lambda = P_\mu = 23.12\,\mathrm{N}$ the membrane is quite "soft", i.e. a light touch of one set of weights or the other can deform the square shape into either one of the two possible rectangles.

[1] Even the data for the inflation and deflation of a balloon are not reliable when the balloon is new. The pressure-radius relation exhibits a "shake-down" upon repetition and a reproducible experiment requires several prior inflation-deflation processes.